

Synthesis and characterization of chiral liquid crystal polymers containing donor–acceptor group

Xiao-Zhi He · Bao-Yan Zhang · Fan-Bao Meng · Mei Tian · Qiang Mu

Received: 23 April 2009 / Accepted: 21 September 2009 / Published online: 18 November 2009
© Springer Science+Business Media, LLC 2009

Abstract A series of new chiral side-chain liquid crystalline polymers with electron donor–acceptor action were prepared containing chiral monomer with donor group and nematic LC monomer with acceptor group. All polymers were synthesized by graft polymerization using polymethylhydrosiloxane as backbone. The mesomorphic properties were investigated by differential scanning calorimetry (DSC), polarizing optical microscopy (POM), thermogravimetric analyses (TGA), and X-ray diffraction measurements (XRD). The chemical structures of monomers and polymers were confirmed by Fourier transform infrared (FTIR), proton nuclear magnetic resonance spectra (^1H NMR and ^{13}C NMR). M_1 did not show liquid crystalline phase and M_2 turned out nematic phase on heating and cooling cycle. Polymers P_2 – P_7 were cholesteric phase. Cholesteric phase and low glass temperature liquid crystalline polymers have been obtained, which offered the possibility of application. Experimental results demonstrated that the glass-transition temperatures rose and isotropization temperatures decreased and the ranges of the mesophase temperature reduced with increasing the content of chiral agent. All of the obtained polymers showed high thermal stability.

Introduction

It is well known that side-chain liquid crystal polymers (SCLCPs) have considerable application potential in the matter of advanced electrooptic technologies. They usually

combined macromolecular characteristics such as mechanical integrity and ease of processability, with the electro-optic properties of low molar mass. Although they response to outside action slowly, a great many SCLCPs with different structures have been reported in the literature due to their potential applied prospect [1–5]. While chiral side-chain liquid crystal polymers, that is, cholesteric or chiral smectic C phases, have been attracted much interest because of unique properties and potential ferroelectric properties [6–17]. Recently, new types of liquid crystalline materials containing chiral groups have been prepared by coordinate bonds, hydrogen bonds, ionic interactions, and electron donor–acceptor interactions. And chiral smectic A polymers had been obtained by introducing chiral and electron donor–acceptor interactions group into polymerization system [17–22]. That is to say, it will be favor for the forming of smectic phase when introducing the interactions between the electron donor–acceptor group. It can be described as follows: The smectic layers were formed by face-to-face acting force between donor and acceptor group in the polymer system, and then the layer accumulated to produce a large region of orientation and the surfaces were built by polarized liquid crystalline unit.

As it is known that the aim of our study generally is to understand the relationship between the molecular structures and the resulting macroscopic material properties. In order to reach this goal, copolymers are often combined by different molecular fragments and give rise to different properties in one material. In copolymer systems, chiral group and electron donor–acceptor group being introduced simultaneously should bring different properties. The aim is to obtain chiral smectic C phase (Sc^*) by utilizing the induced smectic phase and the high rotation power of chiral groups. This kind of electron donor–acceptor interactions cannot be too strong; otherwise it will hinder its

X.-Z. He · B.-Y. Zhang (✉) · F.-B. Meng · M. Tian · Q. Mu
Center for Molecular Science and Engineering, Northeastern University, Shenyang 110004, People's Republic of China
e-mail: baoyanzhang@hotmail.com

responsiveness to outside action, so the unequal length's system has been chosen. In generally, electron donor groups are usually alkyl, alkyloxy, and so on, while electron acceptor groups are usually nityl, nitryl, and so on. The aim of this study is to see the relationship between the electron donor–acceptor interactions and the properties of copolymers, and at the same time, polymers with chiral Sc* phase are expected for the electron donor–acceptor interaction, for the interaction may be favor for molecular arrangement.

In this study, copolymers were obtained by chiral monomer with electron donor group: 6-(4-(allyloxy)benzoyloxy)hexahydrofuro[3,2-b]furan-3-yl 4'-propoxybiphenyl-4-yl adipate (M_1) and nematic liquid crystal monomer with electron acceptor group: 4'-cyanobi-phenyl-4-yl undec-10-enoate (M_2). The influence of chiral agent's contents and electron donor–acceptor action on the polymers' phase behavior is discussed.

Experimental

Materials

Polymethylhydrosiloxane (PMHS, $M_n = 700$ – 800) was purchased from Jilin Chemical Industry Co. (China). Biphenyl-4,4'-diol was purchased from Beijing Chemical Industry Co. (China). 3-Bromoprop-1-ene was purchased from Beijing Fuxing Chemical Industry Co. (China). Isosorbide was bought from Yangzhou Shenzhou new material Co. Ltd (China). 1-Bromopropane was got from Yancheng Longsheng Fine Chemical Industry Co. (China). Ethyl 4-hydroxyl benzoate was purchased from Shenyang Xinxu Chemical Reagent Company (China). Undec-10-enoic acid was purchased from Beijing Jinlong Chemical Reagent Co. Ltd (China). Adipic acid was gotten from Shenyang Longfu Chemical Reagent Company (China). 4'-Hydroxy-biphenyl-4-carbonitrile was obtained from Shijia Zhuang Kangbo industry of fine chemicals. Toluene used in the hydrosilylation reaction was first refluxed over sodium and then distilled under nitrogen. All other solvents and reagents were purified by standard methods.

Measurement

Phase transition temperatures and thermodynamic parameters were determined by using a Netzsch DSC 204 (Netzsch, Germany) with a liquid nitrogen cooling system. The heating and cooling rates were $10\text{ }^\circ\text{C}/\text{min}$. A Leica DMRX (Leica, Germany) polarizing optical microscope equipped with a Linkam THMSE-600 (Linkam, England) hot stage was used to observe phase transition temperatures and analyze LC properties for the monomers and polymers

through observation of optical textures. XRD measurements were performed with a nickel-filtered Cu-K α ($\lambda = 0.1542\text{ nm}$) radiation with a DMAX-3A Rigaku (Rigaku, Japan) powder diffractometer. IR spectra were measured on a Perkin Elmer spectrum one FT-IR spectrometer (Perkin Elmer Instruments, USA). ^1H , ^{13}C NMR spectra (400MHz) were recorded on a Bruker AV400 spectrometer in 5 mm o.d. sample tubes. Specific rotation was performed with Perkin Elmer 341 polarimeter.

Synthesis of monomers

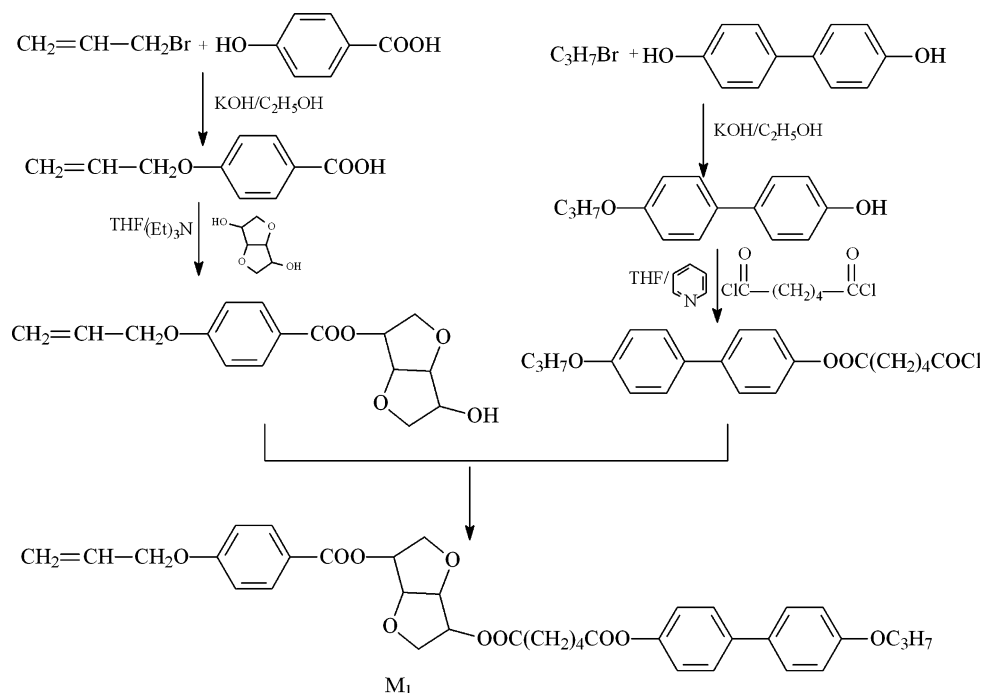
The synthesis route of the monomers is shown in Scheme 1.

Synthesis of chiral monomer: 6-(4-(allyloxy)benzoyloxy)hexahydrofuro[3,2-b]furan-3-yl 4'-propoxybiphenyl-4-yl adipate (M_1)

6-oxo-6-(4'-propoxybiphenyl-4-yloxy)hexanoic acid (precursor) 4'-propoxybiphenyl-4-ol (22.8 g, 0.1 mol) (lab synthesized) solution in 150 mL tetrahydrofuran and 10 mL pyridine was added slowly to a solution containing adipoyl chloride (91.5 g, 0.5 mol) in 100 mL of tetrahydrofuran at room temperature and then refluxed for 15 h. The cold reaction mixture was precipitated into water and acidified to pH = 3–4 with hydrochloric acid. The resulting precipitate was filtered and washed with water to neutrality. The crude product was washed with warm water several times and was recrystallized from the mixture of acetone–ethanol. The white solid powders were obtained. Yield: 68%. mp: $162\text{ }^\circ\text{C}$. IR(KBr): 2980–2850 ($-\text{CH}_3$, $-\text{CH}_2$), 2500–3200 ($-\text{OH}$) 1749 ($\text{C}=\text{O}$ in ester), 1689 ($\text{C}=\text{O}$ in carboxyl), 1605–1450 (Ar–).

6-(4-(allyloxy)benzoyloxy)hexahydrofuro[3,2-b]furan-3-yl 4'-propoxybiphenyl-4-yl adipate (M_1) 6-oxo-6-(4'-propoxybiphenyl-4-yloxy)hexanoic acid chloride (7.4 g, 0.02 mol) in 30 mL tetrahydrofuran was added to a solution containing 6-hydroxyhexa hydrofuro [3,2-b]furan-3-yl 4-(allyloxy)benzoate (8.0 g, 0.026 mol) (lab synthesized) in 30 mL tetrahydrofuran with 3.5 mL pyridine and then stirred 24 h. The resulting precipitate was filtered and washed with water to neutrality. The crude product was recrystallized from ethanol. The yellow solid powders were obtained. Yield: 55%. mp: $105.2\text{ }^\circ\text{C}$, $[\alpha]_{589}^{20} = -64^\circ$. IR(KBr): 3090 ($=\text{C}-\text{H}$), 2980–2850 ($-\text{CH}_3$, $-\text{CH}_2$), 1746, 1727 ($\text{C}=\text{O}$), 1648 ($\text{C}=\text{C}$), 1605–1450 (Ar–), 1258 cm^{-1} ($\text{C}-\text{O}-\text{C}$).

^1H NMR (CDCl_3): δ : 8.02 ~ 6.92 (m, 12H, PhH), 6.08 ~ 6.01 (m, 1H, $\text{H}_2\text{C}=\text{CH}-$), 5.45 ~ 5.25 (m, 2H, $\text{H}_2\text{C}=\text{CH}$), 4.97 ~ 1.79 (m, 12H, isosorbide and $-\text{O}-\text{CH}_2$), 2.67 ~ 1.79 (m, 10H, $-\text{CH}_2-$), 1.09 ~ 1.04 (t, 3H, $-\text{CH}_3$).

Scheme 1 Synthetic routes of monomers M_1 

^{13}C NMR(CDCl_3 , TMS, δ , ppm): 10.3(CH_3), 22.4, 24.0 (methylene-C), 33.5, 33.7($-\text{CO}-\text{CH}_2-$), 68.6, 69.4($-\text{CH}_2-\text{O}-$), 73.3, 73.9, 76.7, 77.3, 80.1 (isosorbide-C), 114.2, 121.5, 127.4 (aromatic tertiary C), 131.6, 132.3, 158.5, 162.4, 165.4 (aromatic quaternary C), 117.9 ($\text{CH}_2=$), 138.4 ($=\text{CH}-$), 171.5 ($\text{C}=\text{O}$).

Synthesis of nematic monomer: 4'-cyanobiphenyl-4-yl undec-10-enoate (M_2)

A few drops of DMF were added to a suspension of undec-10-enoic acid (0.1 mol) in freshly distilled thionyl chloride (40 mL) and the reaction mixtures were refluxed for 10 h and then the excess thionyl chloride was removed under reduced pressure to give the corresponding undec-10-enoyl chloride. Then added it into 4'-hydroxybiphenyl-4-carbonitrile (23.4 g, 0.12 mol) solution with 80 mL tetrahydrofuran and 10 mL pyridine and then refluxed for 18 h. The resulting precipitate was filtered and washed with water to neutrality. The crude product was recrystallized from ethanol. The white solid powders were obtained. Yield: 85%. mp: 51.2 °C. IR(KBr): 2975–2852($-\text{CH}_3$, $-\text{CH}_2$), 2222($-\text{CN}$), 1757($\text{C}=\text{O}$), 1640($\text{C}=\text{C}$), 1605–1450(Ar-), 1258 cm^{-1} ($\text{C}-\text{O}-\text{C}$).

^1H NMR(CDCl_3): δ : 7.24 ~ 8.26(m, 12H, Ar-H), 5.77 ~ 5.87 (m, 1H, $\text{CH}_2=\text{CH}$), 5.03 ~ 4.93(m, 2H, $\text{H}_2\text{C}=\text{CH}-$), 2.58 ~ 2.62(t, 2H COCH), 1.82 ~ 1.34 (m, $-\text{CH}_2-$, 14H).

^{13}C NMR(CDCl_3 , TMS, δ , ppm): 24.4, 28.5, 28.6, 28.8, 28.9, 33.4, 33.9(methylene-C), 113.9($\text{CH}_2=$), 144.0($=\text{CH}-$), 118.4(CN), 121.6, 122.0, 126.2, 127.2, 127.9, 131.4, 132.2 (aromatic tertiary C), 110.6, 136.3, 138.7(aromatic quaternary C), 171.1($\text{C}=\text{O}$).

Synthesis of the polymers

The synthetic route of polymers is outlined in Scheme 2. The mesogenic monomer and chiral agent reacted with Si-H of PMHS to form polymers in the presence of a Pt catalyst. All polymers synthesized are listed in Table 1. The monomers M_1 , M_2 , and PMHS were dissolved in dried, freshly distilled toluene. The mixtures were heated to 65 °C under nitrogen and anhydrous conditions, and then 1.5 mL THF solution of hexachloroplatinate(IV) hydrate catalyst (5 mg/mL) was injected with a syringe. The hydrosilylation reaction, followed the track of the Si-H stretch intensity by FTIR, was completed when the stretch vibrates of Si-H disappeared. The polymers were obtained from methanol, and then were dried in a vacuum at room temperature.

IR(KBr): 2924, 2853($-\text{CH}_3$, $-\text{CH}_2$); 2225($-\text{CN}$), 1755, 1717($\text{C}=\text{O}$); 1606–1450(Ar-); 1200–1000 cm^{-1} (Si-O-Si).

Results and discussion

Synthesis

A chiral agent (M_1), nematic liquid crystalline monomer (M_2), and a series of chiral liquid crystalline polymers containing M_1 and M_2 were prepared. The detailed synthetic routes have been shown in Schemes 1 and 2. M_1 was prepared through the procedure of monoesterification, monoetherification, and esterification and M_2 was obtained by reacting undecanoyl chloride with 4'-Hydroxy-4-biphenyl-carbonitrile. The chemical structures of them

Scheme 2 Synthesis and schematic representation of polymers

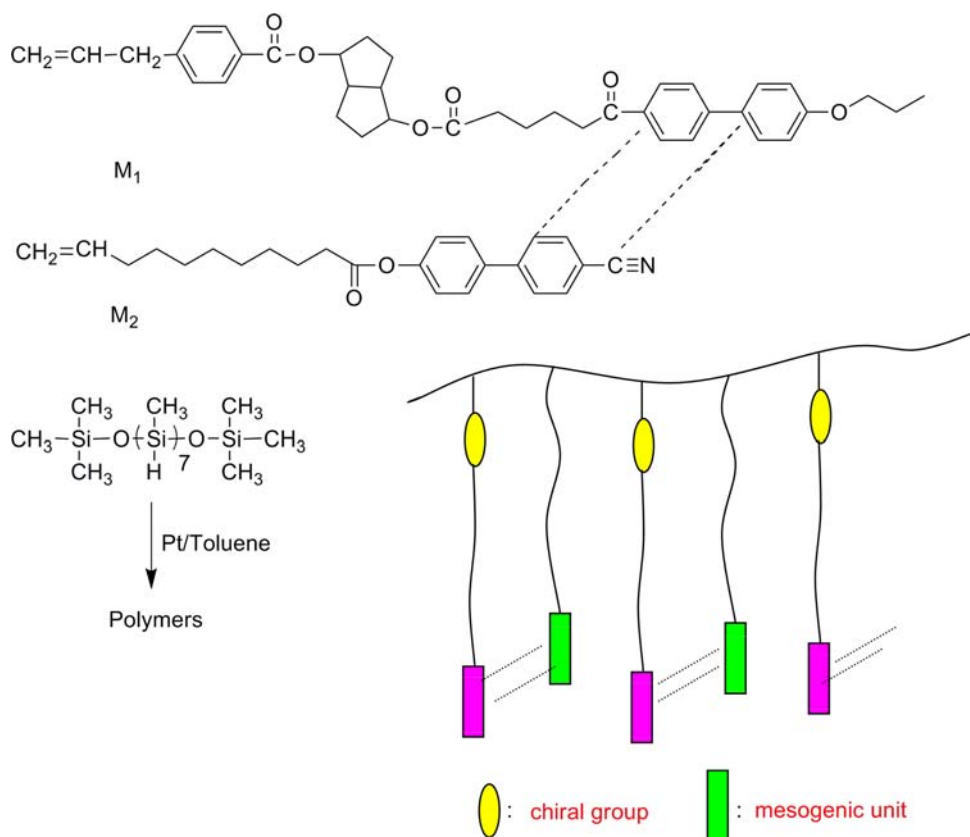


Table 1 Polymerization of $\text{P}_1\text{--P}_7$

Polymer	Feed (mmol)		M_1^a (mol%)	Yield (%)
	M_1	M_2		
P_1	0.000	3.50	0.00	88.2
P_2	0.070	3.43	2.00	83.5
P_3	0.210	3.29	6.00	85.0
P_4	0.350	3.150	10.00	82.6
P_5	0.525	2.975	15.00	83.5
P_6	0.700	2.800	20.00	82.9
P_7	1.050	2.450	30.00	81.3

^a Molar fraction of M_1 based on $\text{M}_1 + \text{M}_2$

were characterized by FTIR, ^1H NMR, and ^{13}C NMR spectroscopy. The FTIR of M_1 and M_2 , respectively, showed characteristic bands at $1757\text{--}1727\text{ cm}^{-1}$ originating from ester $\text{C}=\text{O}$ stretching, $1648\text{--}1640\text{ cm}^{-1}$ due to olefinic $\text{C}=\text{C}$ stretching, and $1605\text{--}1450\text{ cm}^{-1}$ corresponding to aromatic $\text{C}=\text{C}$ stretching. The ^1H NMR spectra of M_1 and M_2 showed multiplet at 6.92–8.26, 5.77–6.08, 4.93–5.45, 4.97–1.97, 1.04–2.67 ppm corresponding, respectively, to aromatic, vinyl, allyl, isosorbide, methyleneoxy, and methyl, methylene protons. IR, ^1H NMR, and ^{13}C NMR spectroscopies confirmed the expected structure and the high chemical purity for these compounds. The

new series of polymers $\text{P}_1\text{--P}_7$ were prepared by a one-step hydrosilylation reaction between Si-H groups of PMHS and olefinic $\text{C}=\text{C}$ of nematic monomer with electron acceptor and chiral agent with electron donor in toluene, using hexachloroplatinate acid as catalyst at $65\text{ }^\circ\text{C}$. The structures of the target polymers are described in Scheme 2. The yields and properties of $\text{P}_1\text{--P}_7$ are summarized in Tables 1 and 2. The FTIR spectra of $\text{P}_1\text{--P}_7$ showed the complete disappearance of Si-H stretching band at 2166 cm^{-1} . Characteristic absorption bands Si-O-Si appeared at $1200\text{--}1000\text{ cm}^{-1}$. In addition, 1755 , 1717 , $1605\text{--}1450\text{ cm}^{-1}$ attaching to the stretching of ester $\text{C}=\text{O}$ and aromatic confirmed that the monomers were introduced into polymer chain successfully. It can be concluded that the chemical structures of monomers and polymers obtained are consistent with our expectation. In appearance, all the polymers are all soft solid due to their low glass temperatures.

Thermal characterization

Analysis of monomer M_1 and M_2

There is only one endothermic and exothermic peak on the DSC heating and cooling curve of M_1 . The two peaks are according to melt temperature ($105.4\text{ }^\circ\text{C}$) and crystallizing point ($66.1\text{ }^\circ\text{C}$). It can be concluded that monomer M_1 has

Table 2 Thermal properties and textures of polymers P₁–P₇

Polymer	$T_g/^\circ\text{C}$	$T_i/^\circ\text{C}$	ΔH (J/g ⁻¹)	ΔT^a	T_G (5%)	LC phase
P ₁	3.3	146.2	4.88	142.9	365.0	N
P ₂	2.2	143.4	4.61	141.2	343.4	Ch
P ₃	3.9	135.2	4.39	131.2	360.3	Ch
P ₄	6.2	131.1	5.69	124.9	350.8	Ch
P ₅	8.5	104.5	4.40	100.0	373.5	Ch
P ₆	9.9	98.5	3.60	88.6	331.2	Ch
P ₇	15.6	97.1	1.95	82.4	314.1	Ch

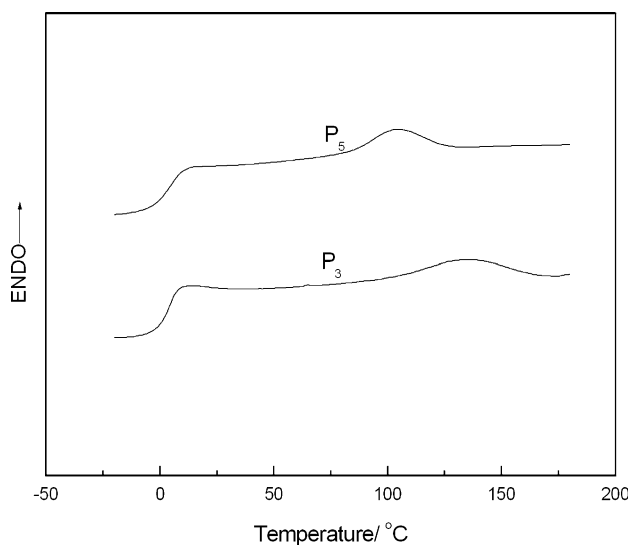
^a Mesophase temperature ranges ($T_i - T_g$)

no properties of liquid crystalline and it is just used as a chiral agent with electron donor group.

There are two endothermal and exothermal peak on the DSC heating and cooling curve of **M**₂. On its heating cycles, a melting transition and nematic–isotropic phase transition for **M**₂ appeared at 50.2, 70.5 °C. On its cooling cycles, the opposite two endotherms of the phase transition can be seen at 67.8, 19.2 °C for isotropic–nematic and crystallization.

Analysis of polymers

Liquid crystalline polymers (LCPs) can be divided into amorphous LCPs, semi-crystallization LCPs, and crystallization LCPs. The range of mesomorphic temperature of amorphous LCP is between the glass-transition and the clearing temperature. Representative DSC curves of polymer, obtained on the second heating scan, are presented in Fig. 1 and phase transition temperature and corresponding enthalpy changes were shown in Table 2.

**Fig. 1** DSC thermograms of liquid crystal polymers

On the second heating scan of polymers, step change and small endothermal are according to glass-transition temperature and mesophase to isotropic phase transition temperature. All transitions are reversible and do not change on repeated heating and cooling cycles, the phase transition temperatures noted in DSC thermograms are consistent with the mesomorphic transition temperatures observed by POM.

It can be seen that the T_g value of polymers is all low, which is due to the flexible chain in the monomers and the existence of nitrile grouping in **M**₂. Nitrile grouping can induce good orientation and reduce the sterical hinder. Low T_g values for LCP are significant as the base of further application.

The influent factors to T_g are summarized as the property of polymer backbone, the rigidity, sterical hinder, and the interaction force between mesogenic and comonomer unit, the flexible spacer length, and the content of comonomer.

Polysiloxanes backbone and mesogenic and comonomer unit with long, flexible spacer incline to reduce T_g value, while hard core of mesogenic and comonomer inclines to increase T_g values. In the present study, the action of chiral non-mesogenic monomer **M**₁ and electron interaction between comonomer should be considered as main factor. The chiral agent may influence the T_g value in two ways. Firstly, may act as non-mesogenic diluent and lead to decrease T_g value; Secondly, isosorbide may introduce sterical hinder to increase the T_g value. While electron donor–acceptor action may withhold free movement of molecular and intend to increase the T_g value. When the two factors were considered at the same time, the glass-transition temperature given by

$$T_g = T_{g0} - K_1\rho_x + K_2A_{D-A}$$

where T_g and T_{g0} are the glass-transition temperature of copolymer and homopolymer, K_1 , K_2 are constant, and ρ_x is the content of chiral agent. A_{D-A} is the proportion of electron donor–acceptor interaction.

At the beginning, T_g values of **P**₁–**P**₂ changed from 3.3 to 2.2 °C which is due to dilution action of chiral agent. But with the increase content of chiral agent, the interacting control between the chiral group's dilution and sterical hinder action and electron donor–acceptor action leads to increase T_g values slowly first and then quickly from 3.9 to 15.6 °C for **P**₃–**P**₇.

The action of chiral agent and electron donor–acceptor not only affected T_g values but also the isotropization temperature (T_i) of LCPs. The chiral agent may affect the T_i values in two ways. On one hand, may act as a non-mesogenic diluent and led to downward shift in the T_i values, On the other hand, heating to the isotropic state required additional energy to distort sterical hinder and led to forward shift in the clearing point. While electron

donor–acceptor interaction may keep liquid crystalline state well and increase the T_i values.

At the beginning, T_i values changed slowly from 142.2 to 131.1 °C for P_1 – P_4 , but then dropped quickly from 131.1 to 98.5 °C for P_4 – P_6 , that is because dilute action is gradually on the leading role with increasing chiral agent's content. And when electron donor–acceptor action is strong enough to counterbalance the dilution of chiral agent, T_i values changed small from 98.5 to 97.1 °C for P_6 – P_7 . The change trends of T_g , T_i and the ranges of the mesophase temperature with different content of chiral agent have been shown in Fig. 2.

Thermogravimetry can explain well about the stability of the polymers. It can show clearly the point and the degree of the polymer decomposition. It can be obtained by TGA. The temperatures at which 5% weight loss occurred (T_d) were greater than 300 °C for P_1 – P_7 , which reveals that the synthesized polymers have a high thermal stability. The TGA curves of polymer are shown in Fig. 3.

LC texture studies The optical texture of monomers and the polymers was obtained by POM with hot stage under nitrogen atmosphere. The visual observations under POM have revealed that M_1 did not exhibit liquid crystalline phase. And M_2 exhibited enantiotropic nematic phase. On the first heating and cooling cycle, it did not turned out characteristic liquid crystalline texture but gorgeous color variation when shearing. On the second heating and cooling cycle, it turned out schlieren and droplet texture for nematic phase. The polymer P_1 showed typical nematic treaded texture. Polymer P_2 – P_7 showed typical cholesteric Grandjean texture on heating cycle and

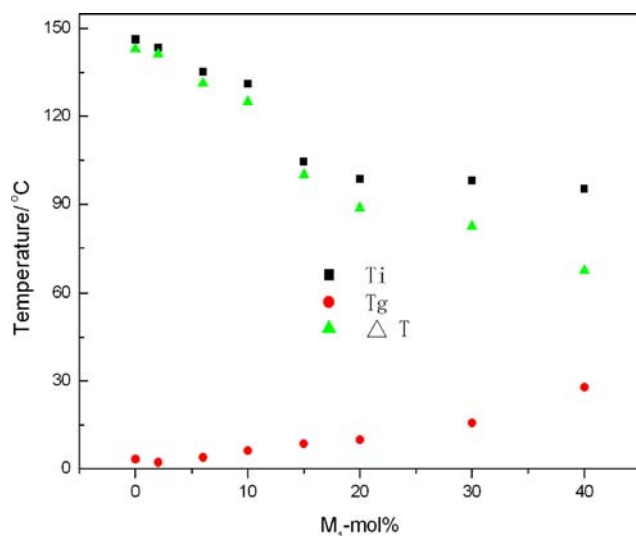


Fig. 2 Effect of M_1 content on phase transition temperature of the polymers

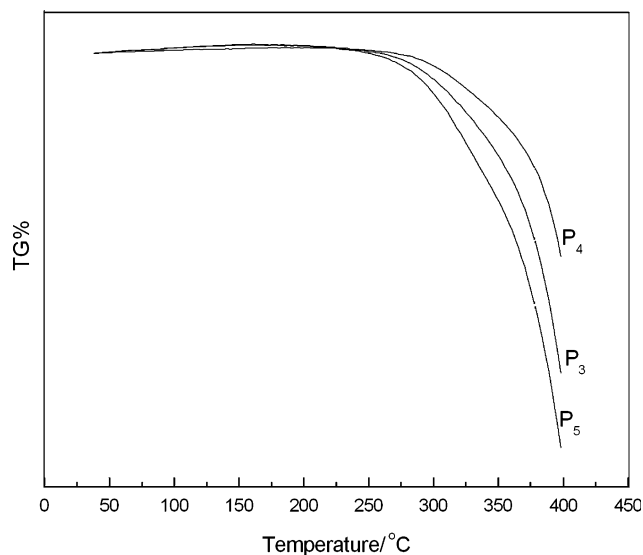


Fig. 3 TGA thermographs of liquid crystal polymers

cholesteric focal conic texture on cooling cycle. It can be seen that the liquid crystalline still existed well when the content of chiral agent is up to 30%. The molecular length of M_1 and M_2 is not equal, so the electron donor–acceptor action is not strong enough. The estimation is proved by gradually subdued liquid crystalline properties. One of the aim of this study is to obtain the chiral Sc phase polymer, but the cholesteric polymers were obtained instead. Perhaps the action of electron donor–acceptor among molecules is not strong enough to ordered molecular arrangement. It can be improved by our subsequent research work. The photomicrographs of monomer and polymer are shown in Fig. 4.

X-ray diffraction XRD analysis allowed for a complementary assessment of the nature of the phases observed by DSC and POM, giving additional information about their structural parameters. In general, a smectic, nematic, cholesteric structure have a broad peak associated with lateral packing at $2\theta \approx 18$ – 25° in wide-angle X-ray diffraction (WAXD) curve which is the distance between the mesogenic side groups. A sharp and strong peak at low angle ($1^\circ < 2\theta < 6^\circ$) in small-angle X-ray scattering (SAXS) curve can be observed for smectic structure which is the smectic layer spacing, but it cannot be seen for nematic and cholesteric structure. X-ray diffraction pattern of the quenched polymer P_1 – P_7 only showed broad peaks at 2θ of 22.68–24.63 ($d = 3.92$ – 3.61 Å). Combining polarizing microscopy with X-ray diffraction measurements may reveal that polymers P_1 – P_7 were cholesteric phase. The representative XRD patterns of polymers were shown in Fig. 5.

Fig. 4 Optical texture of monomer and polymer (200 \times). **a** Color change of M_1 when shearing. **b** Schlieren and droplet texture of M_1 at cooling to 72.5 $^{\circ}\text{C}$. **c** Grandjean texture of P_5 at heating to 71.4 $^{\circ}\text{C}$. **d** Focal conic texture of P_3 at cooling to 135.7 $^{\circ}\text{C}$

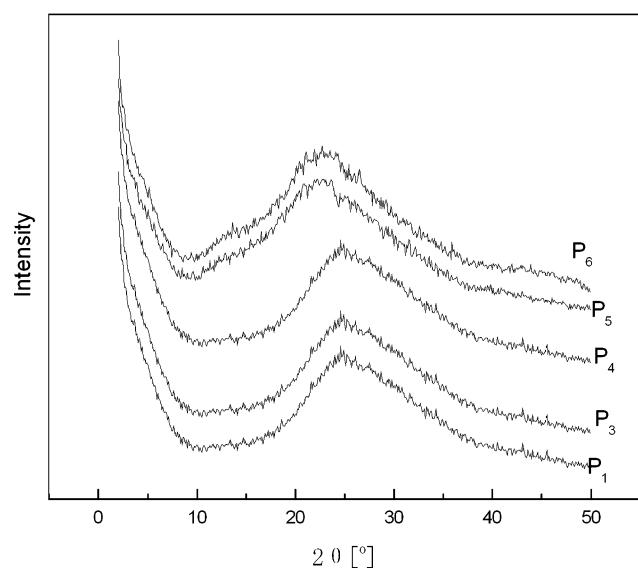
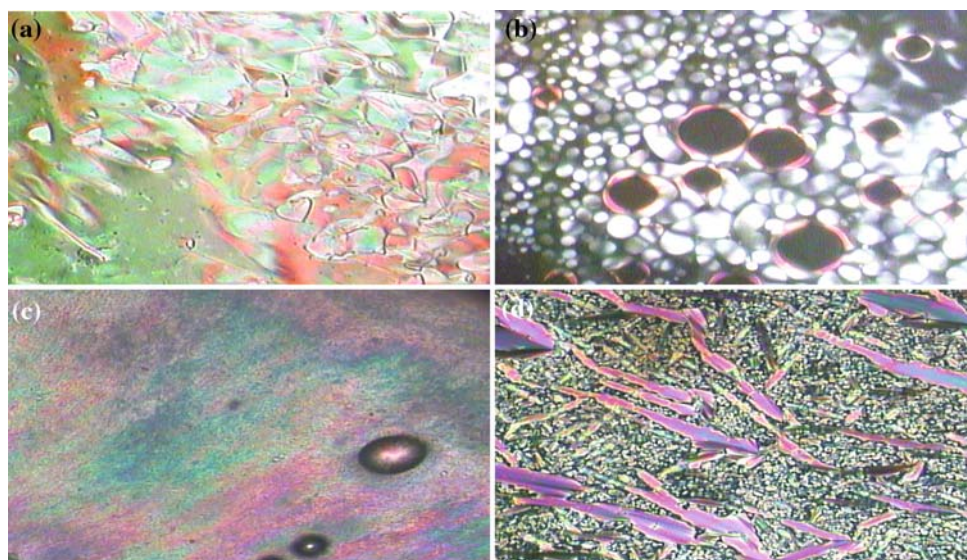


Fig. 5 X-ray diffraction patterns of quenched samples

Conclusions

In this study, a series of new side-chain chiral LCPs with donor–acceptor action have been synthesized and characterized, which came from chiral monomer with donor group: 6-(4-(allyloxy)benzoyloxy)hexahydrofuro[3,2-b]furan-3-yl4'-propoxybiphenyl-4-yl adipate (M_1) and nematic LC monomer with acceptor group: monomer: 4'-cyano biphenyl-4-yl undec-10-enoate (M_2). Cholesteric phase and low glass temperature liquid crystalline polymer have been obtained, which offered the possibility of application. Our aim to synthesize chiral Sc phase did not reach. The subsequent research will be made better under current condition.

Experimental results demonstrated that the glass-transition temperatures rose and isotropization temperatures decreased and the ranges of the mesophase temperature reduced with increasing the content of chiral agent. All of the obtained polymers showed high thermal stability.

Acknowledgements The authors are grateful to National Natural Science Fundamental Committee of China, and HI-Tech Research and development program (863) of China. We also thank National Natural Science Fundamental Committee of China, China Postdoctoral Science Foundation, and Postdoctoral Science and Research Foundation of Northeastern University who all extended financial support of this work. Shen Yang Scientific and Technical Bureau Foundation.

References

- Oriol L, Piñol M, Serrano JL, Martínez C, Alcalá R, Cases R, Sánchez C (2001) *Polymer* 42:2737
- Ansari IA, Castelletto V, Mykhaylyk T, Hamley IW (2003) *Macromolecules* 36:8898
- Cook AG, Imrie CT (1999) *Mol Cryst Liq Cryst* 332:189
- Labarthe LF, Freiberg S, Pellerin C, Pezolet M, Natansohn A, Rocho P (2000) *Macromolecules* 33:6815
- Craig AA, Imrie CT (1999) *Macromolecules* 32:6215
- Kim GH, Jin S, Pugh C, Cheng SZDJ (2001) *Polym Sci Part B Polym Phys* 39:3029
- Shibaev PV, Chiappetta D, Sanford RL et al (2006) *Macromolecules* 39:3986
- Cowie JMG, Hunter HW (1993) *J Polym Sci A Polym Chem* 31:1179
- Bobrovsky AY, Boiko NI, Shaumburg K, Shibaev VP (2000) *Colloid Polym Sci* 278:671
- Taton D, Borgne AL, Chen J, Shum W (1998) *Chirality* 10:779
- Cui ZL, Calderer MC, Wang Q (2006) *Discrete Contin Dyn Syst Ser B* 6:291
- Kricheldorf HR, Sun SJ, Chen CP (1997) *J Polym Sci A Polym Chem* 35:1611
- Broer DJ, Mol GN, Challa G (1989) *Makromol Chem* 190:19

14. Deepa P, Sona M, Jayakannan M (2006) *J Polym Sci A Polym Chem* 44:5557
15. Peter PM (1998) *Nature* 391:745
16. Rebecca AH, Jason MK, Julia AK, Jennifer LH (2008) *J Appl Polym Sci* 110:2914
17. Sahin CMY, Serhatli EI, Menciloglu YZ (2006) *J Appl Polym Sci* 102:1915
18. Fedak I, Pringle RD, Curtis GH (1980) *Mol Cryst Liq Cryst* 64:69
19. Taton D, Leborgne A, Spassky N (1995) *Macromol Chem Phys* 196:2941
20. Kosaka Y, Kato T, Uryu T (1994) *Macromolecules* 27:2658
21. Kato T, Adachi H, Fujishima A (1992) *Chem Lett* 21:265
22. Radano CP, Janssen RAJ, Meijer EW (2004) *Polym Mater Sci Eng* 91:741